M. Aurand

Final Project
12.7.2010
EE554

Abstract

This document outlines the design and implementation of a dual-channel, multiple-input control system for the operation of variable-focal-length lens apparatus.

1. Introduction

Adaptive, or variable-focal-length (VFL) lenses offer significant advantages over conventional glass/plastic lenses. The ability to dynamically adjust focal length potentially reduces the size and complexity of an optical system, while simultaneously providing extraordinary dynamic range.

Conventional optical design mandates the use of fixed-power optical elements, typically made of glass. In order to provide adjustability, the fixed lenses must be mechanically translated relative to each other. A simple example of a variable system utilizing fixed-power lenses is an optical zoom lens or telescope. These systems generally have limited zoom ranges, and require large mechanical displacements to achieve these ranges. Using VFL lenses, mechanical lens translation is no longer required. In addition to mechanical simplicity, optical complexity is reduced as fewer elements are required to achieve the same function as an equivalent fixed-lens solution.

The concept of the variable focal length lens is conceptually simple and has been explored in various forms over the last 10-15 years, with satisfactory performance and versatility still unachieved by industry. This project represents an intense development effort towards convenient, componetized VFL lens technology that provides not only high optical performance, but usability in a variety of applications - “plug-and-play” technology.

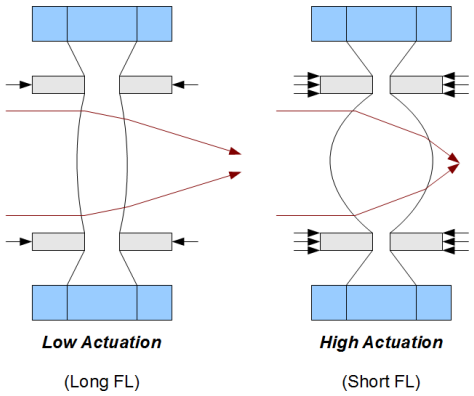

Figure 1: VFL Lens concept. Plungers are pushed into the membranes to redistribute the internal fluid, changing the shape of the active surfaces.

The utilized lens configuration consists of a glass ring, filled with a refractive fluid contained/sealed by two elastic and optically transparent membranes. An actuator system moves plungers in and out of contact with the elastic membranes, altering the curvature of the membrane surfaces. This configuration is mechanically robust and not subject to the leakage problems of hydraulic mechanisms used by other researchers.

Thus, the actuator system must posses several features to make it usable in this configuration. First, the plunger surfaces must be precisely controllable in the direction of movement, and stable in other axes to prevent optical aberrations. The plunger surfaces must move with sufficient repeatability when high loads are present. In addition, the parasitic (holding current) must be very low so battery-powered applications are feasible.

1.1 Requirements

The actuator performance minima can be extracted from the necessary optical characteristics. In order to achieve the desired optical power range (dioptric range > $30m^{-1}$) linear translation distance must be equal to 1.5mm, with a repeatability better than ±4um. Actuation force capabilities must exceed 20N, with a holding force equal or greater than the actuation force. Ideally, the actuator is continuously adjustable, so any desired focal length can be programmed.

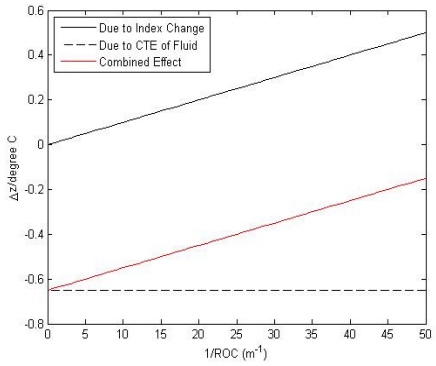

Figure 2: Temperature compensation plot. Two thermal influences are included in this idealized plot, which must be experimentally verified.

The system must also measure and compensate temperature fluctuations. The optical fluid used in the lens has a high coefficient of thermal expansion (CTE), as well as a high change in refractive index over temperature. This specification reduces to the inclusion of a temperature measurement system with a resolution of about 1C, and a fit function to actively move the plungers to maintain any given focal length over a temperature span of 0C to 50C.

2. Background

This section discusses the design and construction of the actual actuator and supporting control system including: component selection, mechanical design, electronics design and software-based closed-loop focal length control system.

2.1 Actuator Design

In order to meet the positional actuation requirements, a unique mechanical driver system is required. Basic evaluation of common linear actuator solutions reveals nothing meeting all of the system requirements acceptably. These common solutions include piezo stacks, piezo "leg" actuators, solenoid-systems, and conventional DC motors (brushed, brushless and stepper). Because the direct-linear actuators lacked the force/volume efficiency required, the viable solution space shrank to rotary-type motors with a threaded rotary-to-linear mechanical conversion stages. Solutions using brushed DC motors were tested and successfully demonstrated, however, in order to meet packaging and temporal requirements the motors were over-driven and therefore became unreliable (failure was common). In addition, the rotary-to-linear conversion was very inefficient as initially designed (too many threads actively engaged) and this led to serious problems with material wear – eventually causing repeatability issues.

In search of a more ideal solution, the ultrasonic ring motor (USM) was investigated. Inspiration came from a Canon DSLR lens assembly which utilized a similar technology. From a physical form-factor perspective, this motor was optimal as it has a central hole through which light can pass, and high-torque characteristics which eliminate the need for gear reduction. The USM unfortunately requires a specialized quadrature high-voltage sinusoidal drive technique, which complicates the electronic design. It was decided that the mechanical advantages outweighed the electronic complexity, and the USM was optimized for the VFL lens application.

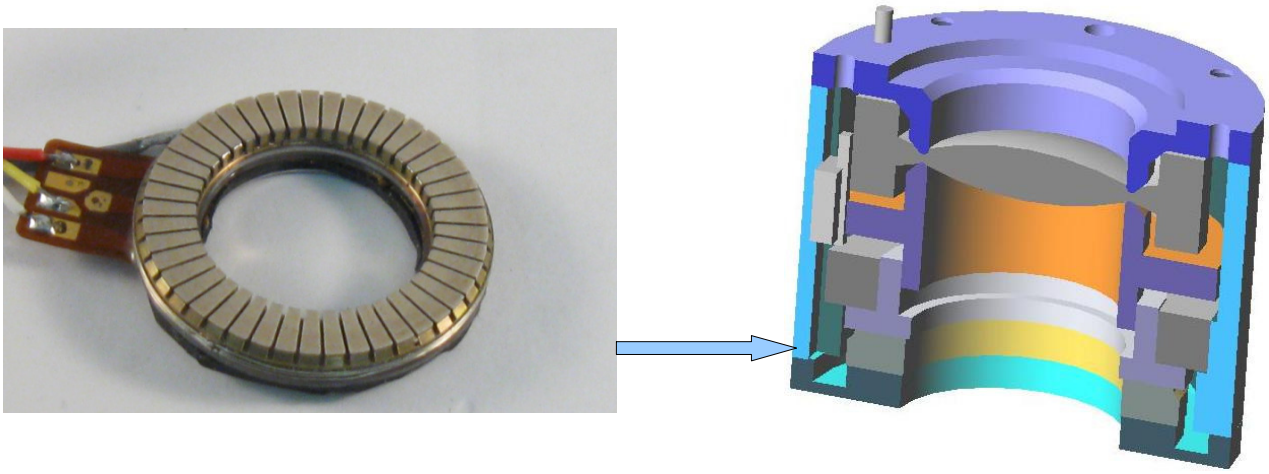

Figure 3: USM actuator integration. The motor stator is shown in the CAD model as yellow, with the moving rotor shown above it in gray. The purple section threads into the revolving rotor, providing the linear motion required to actuate the lens core.

An off-the-shelf Shinsei motor was modified to fit the system requirements. This modification entailed the design of a new rotor system with threaded rotary-to-linear conversion stage. In addition, the center of the stator was bored out to the required clear aperture of the VFL lens core to avoid optical vignetting. The motor was integrated into a complete mechanical design that included a linear position sensor for closed-loop position control of the plunger system.

2.2 Position Sensing

In order to meet the required 4um position repeatability requirements, a high-accuracy encoder system was required. Initially, optical grating-based sensors seemed optimal, but their mechanical configurations and relatively large dimensions did not easily allow their use. Fortunately, MicroStrain

manufactures miniature position sensors that provided the necessary form factor. These are of the differential variable-reluctance transducer (DVRT) design with many details ideally suiting it to the system at hand.

First, the transducer is an absolute type which removes the need for the initialization and indexing routine that would be required for an incremental encoder type (primarily optical). This sizable advantage was combined with an extraordinary compact physical size. The monetary cost of these advantages is quite high, as the sensor itself sells for approximately $1500. The complexity of the required interface electronics also far exceeds those mandated by an optical encoder.

Two signal conditioning approaches were investigated to accompany this sensor system. A NMT-designed electronics package was tested, as was a very expensive ($3000) COTS solution. Both met physical size and power-consumption requirements, but the COTS electronics had better electrical performance from a noise standpoint. The COTS system provides a usable resolution of 12-bits, while the NMT hardware was a factor of 2 less resolute. The COTS system was chosen in the end, but the NMT electronics are being optimized as they are superior in terms of power consumption and solution size.

2.3 Control Hardware Architecture

Upon finalization of actuator mechanisms and electronic requirements, a specialized integrated electronic controller was designed. This design allows the connection and control of two independently operable VFL units.

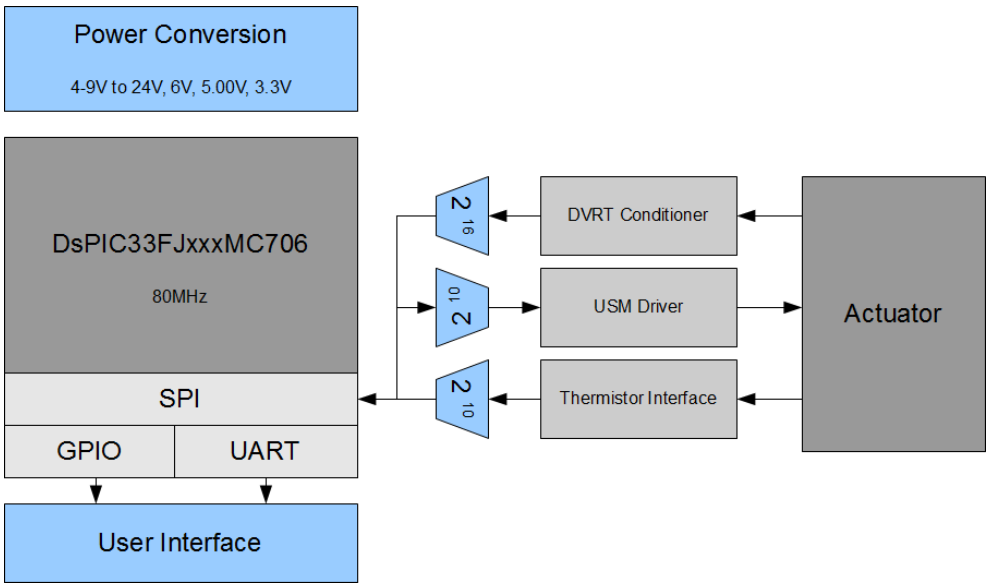

Figure 4: Overall system block diagram showing critical hardware components.

2.3.1 Controller

The controller chosen was a high-performance microcontroller. There are many potential devices that would work for this application (it is not a particularly demanding application), including those from TI, Cypress, Atmel, Motorola and Microchip. The selected device was a dsPIC33FJ128MC706A by Microchip. This device was selected as it had adequate GPIO, 12-bit on-chip ADC and development

software/hardware was readily available. In addition, the sytem designer is very familiar with these parts to facilitate rapid software design.

The controller operates at 80MHz (or 20MIPS). Control loop update rate is 2kHz, slightly faster than the maximum motor halt latency of 1ms and approximately equal to the bandwidth of the position sensing circuitry.

2.3.2 ADC

The control system requires two digitized inputs; temperature and position for each of two controlled actuators. To fulfill these requirements, ADCs were selected for each input device.

2.3.2.1 Positional Conversion

To enable future improvements in DVRT signal conditioning hardware, a dual-channel low-power 16-bit ADC was selected that meets the necessary interface requirements. This ADC is operated at 8kHz, with 4 conversion results averaged for each position loop controller iteration. This reduces random read/sensor noise while not negatively affecting the control system (the averaged sample rate of 2kHz is comparable to the conditioning hardware bandwidth to ensure stability).

The ADC has a specified conversion error of ±3LSBs, generating an ENOB of slightly better than 14-bits. In software, the result is truncated to 12-bits to generate a noise-limited positional measurement in increments of 1.5um (~3x less than required 4um). The ADC is provided with a precision voltage reference and dedicated low-noise power supply to eliminate excessive noise introduction and improve accuracy over time and temperature.

2.3.2.2 Temperature Conversion

Temperature must be measured for active athermalization. The sensor that met accuracy and size requirements over the operation temperature range is a 10K (@25C) thermistor. While a discrete signal conditioning solution was investigated, it was found to have unnecessarily high resolution at the expense of power consumption. A monolithic solution was discovered (MAX6682) which has very low power consumption, an integrated ADC and first-order linearization. This solution was selected and optimized for the operational temperature range of 0C to 50C, giving resolution of better than 0.1C. This device is quite slow (100ms/sample), which is acceptable as the temperature fluctuations of the lens fluid have a very high time constant (>10s).

2.3.3 DAC

The DAC drives the USM. At the moment, the Shinsei COTS motor driver board is utilized, which requires several logic-level binary interface lines, as well as an analog speed setpoint input (0 to 3.2V). This COTS driver is essentially a quadrature voltage-to-frequency converter that is transformer-coupled to the USM to generate the high drive voltages necessary. By changing the drive frequency, a mechanical traveling wave is induced in the stator, allowing variation in rotational velocity.

A dual 10-bit converter was selected due to higher-than-required resolution, small package, low power-consumption and integrated output buffer amplifiers (eliminating the need for external buffer amplifiers). This part easily operates at the required 2kHz loop rate.

The interface was designed to also support an NMT-developed USM high-voltage driver. This driver was not used in this iteration due to time constraints, although it has been successfully demonstrated, displaying higher efficiency and packaging flexibility than the COTS unit.

2.4 Control Software Architecture

The software of the controller resides in the 80MHz PIC microcontroller. In addition to housekeeping functions, the high-priority control loop is executed when triggered by a 8kHz/4 timer interrupt.

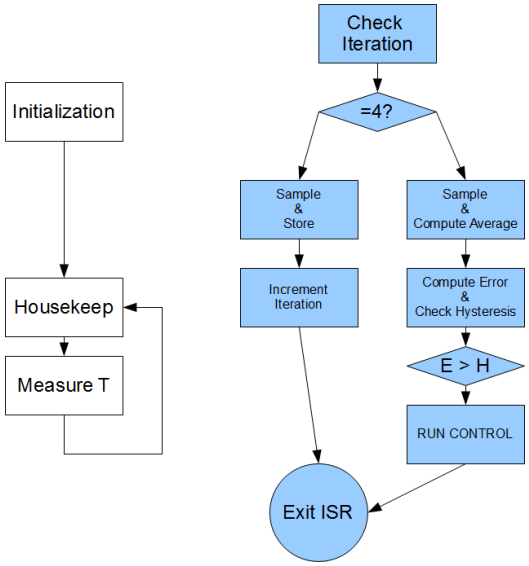

Figure 5: General firmware operation diagram.

2.4.1 Housekeeping

The housekeeping functions include handling user interface commands and status indicators, as well as measurement of temperature. This loop runs at a rate of approximately 10Hz, as temperature time constants are very high (>10s). The temperature compensation is a simple linear function that adjusts the plant position setpoint according to both desired focal length and current temperature.

2.4.2 ISR Control Loop

The interrupt-driven control loop runs at a rate of 2kHz, providing more than adequate temporal resolution compared to the motor response. The ISR collects and averages four individual 16-bit samples at a rate of 8kHz, truncates the 12-bit usable result, and checks to see whether or not the actuator position is within the acceptable hysteresis deadband. If the position is within the hysteresis bounds, the control will hold the current position to minimize idle current consumption. If the error is large, however, the controller will be run until the new setpoint is reached.

2.5 The Control Algorithm

The USM-based actuator system has several unique constraints and properties that conspire to inhibit the implementation of a good controller (especially a PID type).

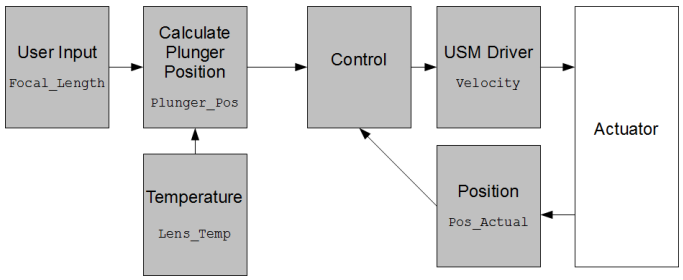

Figure 6: Control system flow diagram. User input is a focal length, which is mapped to a plunger position plant variable (that is a function of temperature), while the plant output is a controlled plunger position.

Deadband

The velocity deadband of the USM system varies with actuation distance and motor temperature. At no load, the entire range of velocities is attainable, while at high loads a narrow range of setpoints actually work. This is likely due to motor mechanical preload increasing as actuation force is applied. This is very difficult to characterize, but basic measurements were taken to determine operational speeds at different points within the actuator travel.

Stall Detection

The motor operates by mechanical resonance, and drive frequency is altered to induce a traveling wave in the stator upon which the rotor rides. This drive frequency is dithered to maximize mechanical deflection. Upon stalling, the frequency must be increased then re-dithered to get a reliable movement. The startup process takes about 100ms.

Differing Start/Stop Time Constants

The stop time constant of the USM is extremely low (millisecond period), but the startup time is on the order of 100ms.

Velocity Non-linearity

Velocity vs. setpoint of the motor system is very non-linear, changing dramatically as load forces vary.

2.5.1 Characterization Summary

Characterization of the USM actuator system is very difficult due to small travel range, high transit speeds and severe motor difficulties. In the end, it was found that slowly ramping the velocity on startup was mandatory for repeatable and reliable operation – simply applying a "go" command frequently results in failure, especially at the actuation extremes. Stopping the motor is nearly instantaneous, a feature exploited by the current controller configuration to obtain high settling precision. The usable "linear" range of the motor is small and highly dependent on current position.

2.5.2 Controller Attempts

At first, a simple "bang-bang" type control was attempted to verify basic system operation and determine operational parameters. This algorithm simply started the motor and stopped it when the desired position was reached (within hysteresis band). It was discovered that the motor did not start or

settle reliably – this most trivial controller was unsuitable, as expected.

Next, a PID controller was implemented. The PID controller had better response but tuning was difficult due to gross changes in motor performance over the actuation range. Either the system would be severely under-damped at the high actuation state, or oscillation [even runaway] would occur at the low actuation state. Another issue was the idle power consumption. With an adequate integral term to overcome the variable deadband, the motor would often remain "on" at a low velocity setpoints, which generated no motion and merely consumed large amounts of power. Several methods were used to attempt to solve the basic issues, including: position-dependent deadband offset, hysteresis shutoff, and adaptive PID coefficients. While satisfactory responses were obtained with the modified PID controller algorithm, the output was simply not dependable. It would often work well for a few hours in the morning, and upon return from lunch or dinner the same configuration would fail to operate. This was traced back to thermally-induced motor variations, but in any case a more robust algorithm was required.

Trajectory control promised to solve at least the startup issues, as the motor could be ramped up to a reliable velocity. Unfortunately, PID coefficients were still not sufficient to guarantee operation without multiple starts/stops per requested transit.

The best results were observed with a much simpler controller. The final controller is a linear-only state-machine-based implementation of a trajectory generator. The state of the system (low, medium or high actuation) dictates the low-speed limits of the motor and deceleration coefficients. Upon a request for translation, a ramp function is sent to the motor to get it spinning, stopping acceleration when a maximum velocity (user-set) is reached. Depending on the desired setpoint, a deceleration is initiated when the actuator is near the desired endpoint. The motor is simply shutdown immediately when the setpoint is reached. This controller takes advantage of the rapid shutdown/locking capabilities of the USM.

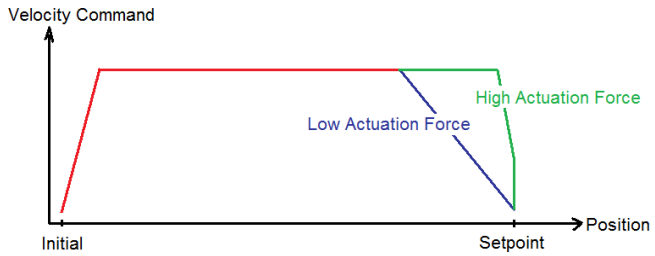

Figure 7: Demonstrates trajectory controller operation. The final deceleration knee and deadband is dependent on the positional properties of the setpoint.

Stall detection is implemented to warn the user of stall/jam conditions, as well as automatically attempt to clear the stall. This ensures consistent and trustworthy operation.

3. Results

Despite the simple control algorithm (in retrospect – achieving the controller was non-trivial) the results are more than acceptable.

The lens can be reliably actuated over its entire operational travel range of 1.5mm linear travel (corresponding to a dioptric range of $30m^{-1}$). Reliability is one of the primary concerns, second only to positional accuracy. Positional accuracy is very good (um level) but a non-trivial thing to test (a human hair is about 50um in diameter). Transit time depends on the maximum velocity setpoint, and averages 0.7s (measured by oscilloscope).

Advanced repeatability testing was needed to verify satisfactory operation. Independent (not utilizing the DVRT process monitor) validation is required to verify the optical properties of the complete system. Single-pass interferometric testing using a shear plate indicated that the repeatability was in the ballpark of the 4um specification, but this testing does not produce valid quantitative results.

For high-precision measurements, a Zygo interferometer was used to verify the focus error due to actuator inconsistencies. The test configuration utilized high accuracy reference elements (λ/20) and double-pass configuration to exaggerate the error to be tested (by a factor of two).

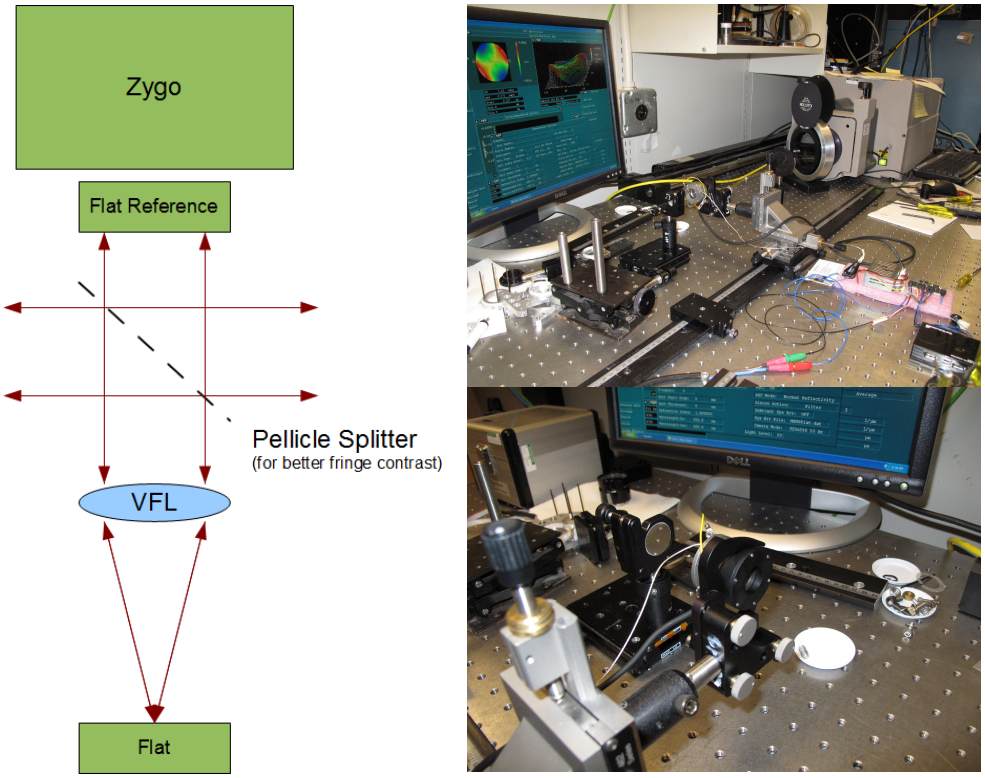

Figure 8: Optical testing setup. The VFL is actuated between several points to verify settling accuracy at any particular test power. Defocus error was analyzed to produce linear plunger error figures.

The standard deviation of the systematic plunger error was computed as 1.145um from a total of 80 trials at 3 different focal ratios. This verifies that the positional error is comparable to the electrical position measurement noise (1.5um), and that the system is operating to the limits of the hardware.

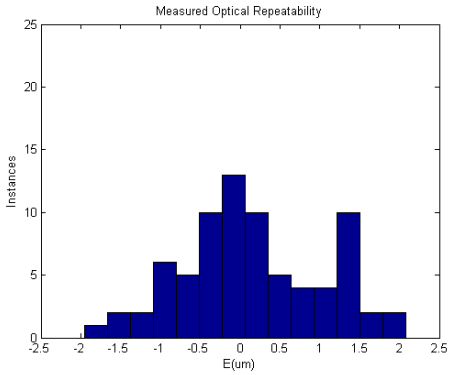

Figure 9: Histogram of repeatability results, N = 80, σ = 1.1448.

Figure 9 demonstrates the repeatability results. There is a prominent second bar at an error of ~1.5um, which is equal to 1 count of the DVRT, attributed to the pressure-induced settling of the actuator plunger at high loads when the USM is powered down, within the hysteresis band of ±1 count.

4. Summary

The actuator and controller work well, meeting and exceeding all required specifications. At the moment, temperature characterization and compensation have not been completed, but will be finalized in the next 8 weeks.

PID control of non-linear systems is difficult, and presented issues that compounded the complexity greatly. By taking a step back and re-assessing the capabilities and limitations of the USM, a much simpler controller design was enabled. This simple state-machine-type controller provides better overall performance with no decrease in positional resolution or accuracy.